HINDCAST OF TYPHOON JONGDARI AND NON-TIDAL SEA LEVEL RESIDUALS IN MIKAWA BAY USING FDDA IN WRF

RYO NAKAMURA
Toyohashi University of Technology, Toyohashi, Aichi, Japan, ryo-nakamura@umi.ace.tut.ac.jp

KYEONG OK KIM
Korea Institute of Ocean Science & Technology, Busan Metropolitan City, Korea, kokim@kiost.ac.kr

SHIGERU KATO
Toyohashi University of Technology, Toyohashi, Aichi, Japan, s-kato@ace.tut.ac.jp

RYOTA NAKAMURA
Niigata University, Niigata, Niigata, Japan, r-nakamura@eng.niigata-u.ac.jp

TAKUMI OKABE
Toyohashi University of Technology, Toyohashi, Aichi, Japan, okabe@ace.tut.ac.jp

ABSTRACT

Numerical simulation of the storm surge by an unexpected typhoon and the elucidation of the mechanism of its occurrence are indispensable for improving disaster prevention measures in coastal area. Reproducibility of meteorological fields such as wind speed and atmospheric pressure by a typhoon is important for estimating storm surge. For improving the reproducibility, four-dimensional data assimilation (FDDA) is applied in Regional Climate Model. Numerical simulation of storm surges caused by typhoons, for examples, Isewan Typhoon that caused enormous damages in coastal area of Ise and Mikawa Bays in 1965, has been carried out, and the mechanism of its occurrence also has been investigated by many researchers so far. Typhoon Jongdari in 2018 approached to the mainland of Japan. However, its track was from east to west, which is an opposite direction of the typical typhoon track around Japan. The effectiveness of FDDA on the hindcast of Typhoon Jongdari and the reproduction of anormal water level deviation in Mikawa Bay were evaluated using atmospheric model, WRF, and ocean flow model, FVCOM. The lowest atmospheric pressure, the maximum wind speed and the sea level departure by storm surge were analyzed. The spectrum nudging in WRF demonstrated the results with higher accuracy than those by grid nudging or no nudging.

Keywords: typhoon hindcasting, four-dimensional data assimilation, storm surge, WRF, FVCOM

1. INTRODUCTION

Frequent coastal disasters due to strong wind and flood occurred by typhoon and storm surge in Ise Bay and Mikawa Bay. Numerical simulation of storm surges in their bays caused by typhoons such as Typhoon Vera in 1965, which is called Isewan Typhoon, and Typhoon Melor in 2009, has been conducted by many researchers to investigate the mechanism of its occurrence so far (e.g., Kato et al., 2014; Murakami et al., 2013). Around Japan, typical track of a typhoon including Typhoon Vera and Melor is from west to east. However, the trajectory of Typhoon Jongdari (July 2018) is from east to west, which is an opposite direction to the typical track. Therefore, it is called "reverse run typhoon" in Japan. Its strength is weaker and the damage was smaller than Typhoon Vera and Melor. However, Typhoon Jongdari also had the possibility of generating big storm surges, as in the case of Hurricane Lenny. This hurricane occurred in the Caribbean in November 1999 with the “reverse track”, and the casualties were 17 killed, the total economic damage was amounted to 330 million dollars (Guiney, 1999). The numerical simulation of storm surges for coastal disaster prevention and mitigation has been conducted using the typhoons which track was assumed based on the historical severe typhoon disaster. Typhoon Jongdari is the first record of the reverse track as from east to west on Japan. Therefore, numerical simulation of the storm surge generation by the typhoon with unexpected tracks and the investigation of its mechanism are indispensable for improving coastal area disaster prevention measures.

Reproducibility of meteorological fields such as wind speed and atmospheric pressure is important in estimating storm surges. In the past, the empirical typhoon model was used to calculate air pressure and wind speed for the storm surge simulation (e.g., Myers et al., 1961). In this model, the influence of the topography for meteorological condition is not considered. However, the use of objective analysis data by Global Climate

Model which has been improved in accuracy and resolution and meso-meteorological analysis result by Regional Climate Model has become the major method for the storm surge simulation. Yasuda et al. (2008) calculated the storm surge and the tide level fluctuation in the Seto Inland Sea using WRF (Weather Research and Forecasting model). The prediction result shows that the water level rises due to the storm surge using WRF can be reproduced with high accuracy than those using the typhoon model. In addition, Yasuda et al. (2009) shows the WRF simulation with the nudging calculation using analytical values only in the first area and the nesting calculation for the smaller areas can obtain the most accurate result in the storm surge simulation. They simulated the typhoon with typical track and its storm surge. However, few attempts have been made to improve the reproducibility of simulation of storm surge generation by the typhoon with unexpected tracks. Therefore, the reproducibility improvement of numerical simulation of the storm surge generation by the typhoon with unexpected tracks is indispensable for the advanced investigation of its mechanism.

In this study, we examined the effectiveness of four-dimensional data assimilation in the atmospheric model on the reproduction of Typhoon Jongdari and its storm surge deviation.

2. MODEL DESCRIPTION

2.1 Simulation Model

First, WRF estimates wind velocities at 10 m above sea level and sea level pressures. Then, the results of these atmospheric fields near ocean surface are used as the initial and boundary conditions in FVCOM (Finite Volume Community Ocean Model, Chen et al., 2003), in order to reproducing the non-tidal sea level residuals.

The WRF system contains two dynamical solvers, referred to as the ARW (Advanced Research WRF; Skamarock et al., 2008) core and the NMM (Non-hydrostatic Mesoscale Model; Janjic, 2003) core. It is a fully compressed non-static model and excels meteorological simulation across scales ranging from tens of meters to thousands of kilometers. Further, it includes latest physics models (cumulus physics, radiation, land surface, planetary boundary layer, etc.). ARW is created from MM5 model in NCAR and has much more complex dynamic and physics settings than NMM. Moreover, it includes data assimilation system. NMM is created from ETA model in NCEP and calculated much faster than ARW. In this research, ARW was used.

FVCOM is a prognostic, unstructured-grid, finite-volume, free-surface, 3-D primitive equation coastal ocean circulation model. This model consists of momentum, continuity, temperature, salinity and density equations. It is closed physically and mathematically using turbulence closure models such as $k-\varepsilon$ model and MY (Mellor-Yamada)-2.5 turbulent closure model. The horizontal grid is comprised of unstructured triangular cells. Thereby, outer grids are generated along coastal line. The sea floor is reproduced using Sigma coordinate system. FVCOM Version 4.1 was used in this study.

2.2 Data Assimilation Methods

Four-dimensional data assimilation (FDDA), also known as nudging, is a method to minimize the difference between the simulated estimation and the observation by introducing forcing term to basic equations in both time and space. WRF has the grid nudging and spectral nudging.

Nudging can be applied to the two horizontal wind components (u and v), temperature and specific humidity. The method is implemented through an extra tendency term in the nudged variable's equations. The basic equations including forcing term are set as below,

$$\frac{\partial \mu \alpha}{\partial t} = F(\alpha, x, t) + G_\alpha W(\hat{\alpha}_0 - \alpha) + G_\mu W(\hat{\mu}_0 - \mu) \quad (1)$$

Here, $F(\alpha, x, t)$ represents the normal tendency terms due to physics, advection, etc., α is wind components (u or v) or temperature or specific humidity, μ is difference air pressure between upper air and surface, G_α and G_μ are timescales controlling the nudging strength, W is an additional weight in time or space to limit the nudging, while $\hat{\alpha}_0$ and ρ_0 are the time- and space- interpolated analysis field value towards which the nudging relaxes the solution. The grid nudging is most common technique. The atmospheric model is nudged towards time and space interpolated analyses using a point-by-point relaxation term. On the other hand, the spectral nudging nudges only selected larger scales of phenomena and allows a model to evolve small scales phenomena without nudging.

3. EXPERIMENT DESIGN

3.1 Model domains

The computational domains in this research are shown in Figure 1. In the typhoon simulation, the large domain and the small domain are connected by nesting technique. The center of domain 1 is Ise Bay and Mikawa Bay. These domains cover wide range to encourage enough growth Typhoon Jongdari within them. The calculation area in FVCOM is Mikawa Bay, Ise Bay, and Northwest Pacific Ocean near there. Domain size is shown in

Table 1. Unstructured bathymetric data for storm surge simulation by FVCOM is reconstructed from structured grid data provided by Central Disaster Management Council (2016) for Nankai Trough Earthquake Tsunami simulation.

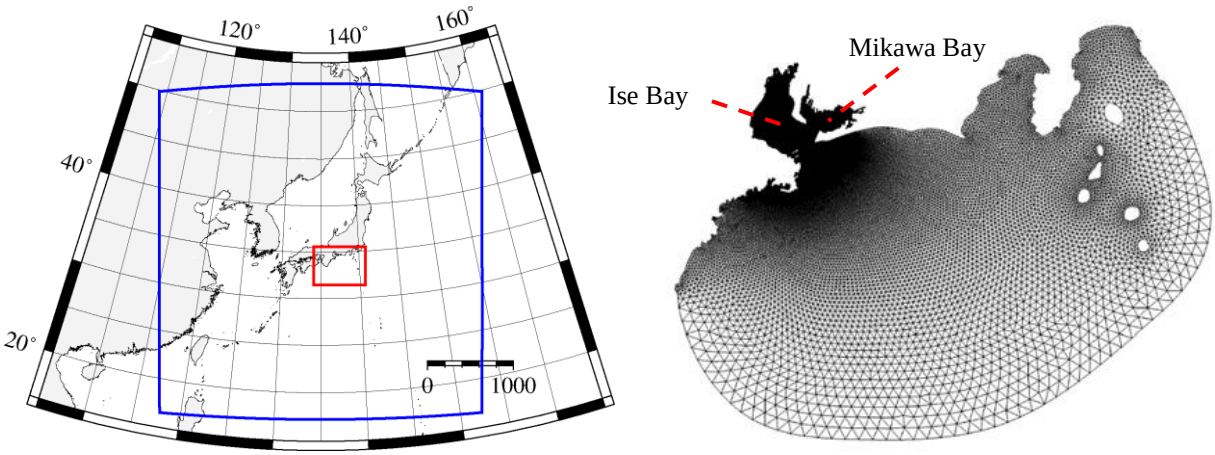

(a) WRF area (blue: domain 1, red: domain 2) (b) FVCOM domain

Figure 1. The calculation areas

Table 1. Domain information

WRF		FVCOM	
Map projection	Lambert	Number of node	56414
Number of horizontal grid	Domain1: 250×250 Domain2: 121×91	Number of cell	107926
Grid size	Domain1: 15km Domain2: 5km	Grid size	50m ~ 10000m
Number of vertical layers	32	Number of vertical layers	10

3.2 Typhoon Jongdari (201812)

Typhoon Jongdari occurred at 3:00 JST 25th July, 2018 at 20°20'N and 136° 35'E with the minimum pressure of 960 hPa and the maximum wind speed of 40 m/s. Its track was from east to west and it was the opposite direction against the typical typhoons, as mentioned in "1. INTRODUCTION".

Figure 2 shows Jongadri track. Jongdari moved from east to west on the southern coast of the main island of Japan. It landed in the west of Japan. After, it reached China.

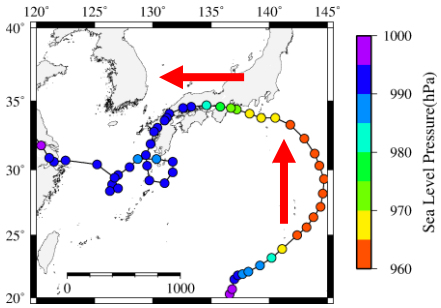

Figure 2. Jongdari track

3.3 Simulation Cases

By changing the calculation condition of WRF, optimal weather model conditions for storm surge estimation were examined. Conditions are as follows:

NN: Not carrying out 4-dimensional data assimilation analysis,

GN: Using grid nudging objective analysis data in the first area,

SN: Using spectrum nudging objective analysis data in the first area.

4. RESULTS

4.1 Initialization

Calculation period is from 6:00 UTC 27th July 2018 to 6:00 UTC 30th July 2018 in meteorological and storm surge simulations. In Domain 1, time interval for simulation is 30 seconds and in Domain2, 10 seconds. FNL (Final) Operational Global Analysis (time interval: 6 hours, grid interval: 1 degree, vertical layer: 32 layers; UCAR, 1999) were used for initial condition, boundary condition and 4-dimensional assimilation data. Selected physics schemes are shown in Table 2. Implicit Gravity Wave Radiation was used as open boundary condition in FVCOM. The wind-stress coefficient C_D of the air-ocean interface was based on Wu (1980) with the limitation of 0.03 (Powell et al., 2003).

$$C_D = (0.8 + 0.065 \times W_s) \times 10^{-3} \quad (2)$$

$$C_D = 0.03 \qquad if \qquad C_D > 0.03 \quad (3)$$

Here, W_s is wind speed (m/s) at 10m above sea level.

Table 2. Physics schemes in WRF

List	Options, scheme
Micro Physics	WRF Single–moment 6–class
Cumulus Physics	Kain–Fritsch
Longwave Radiation	RRTM
Shortwave Radiation	Dudhia
PBL Physics	Yonsei University
Surface Layer	Revised MM5
Land Surface	Unified Noah Land Surface Model
Urban Physics	N/A

4.2 Typhoon track and intensity

Figure 3 shows the typhoon tracks of WRF results (NN, GN, SN), Best Track (JMA) and FNL. Around Japan, GN is the closest to JMA and NN is the most different in the western part of the mainland after landing (Figure 3 (a)). After crossing Kinki district, JMA passes through the south part of Chugoku region and reached the north part of Kyushu from northeast to southwest. The result of GN demonstrated the similar track to JMA although passing slightly south. The track of SN passes further south than those of JMA and GN. In contrast, the track of NN passed north of JMA, and reaches Japan Sea. Near Ise Bay and Mikawa Bay, GN is close to the best track (Figure 3 (b)).

The maximum wind speed of the typhoon is shown in Figure 4. SN is closest to JMA. NN is also similar to JMA by 12:00 29th July, but after that time, it overestimates than JMA. Wind speed by GN fluctuates in the cycle of about 6 hours in the first 24 hours. It is because data assimilation by grid nudging is implemented using FNL which is updated every 6 hours. In every case, there are large decreases in the wind speeds between 12:00 and 18:00 28th July. These are caused by the typhoons landing (Figure 3 (a)). Wind speed by JMA declines by about 5m/s. Wind speed by GN declines by 6 m/s. The changes of wind speed are almost same. However, the wind speed (strength) of GN is lower about 10 m/s than that of JMA. Then, it was made clear that reproducibility

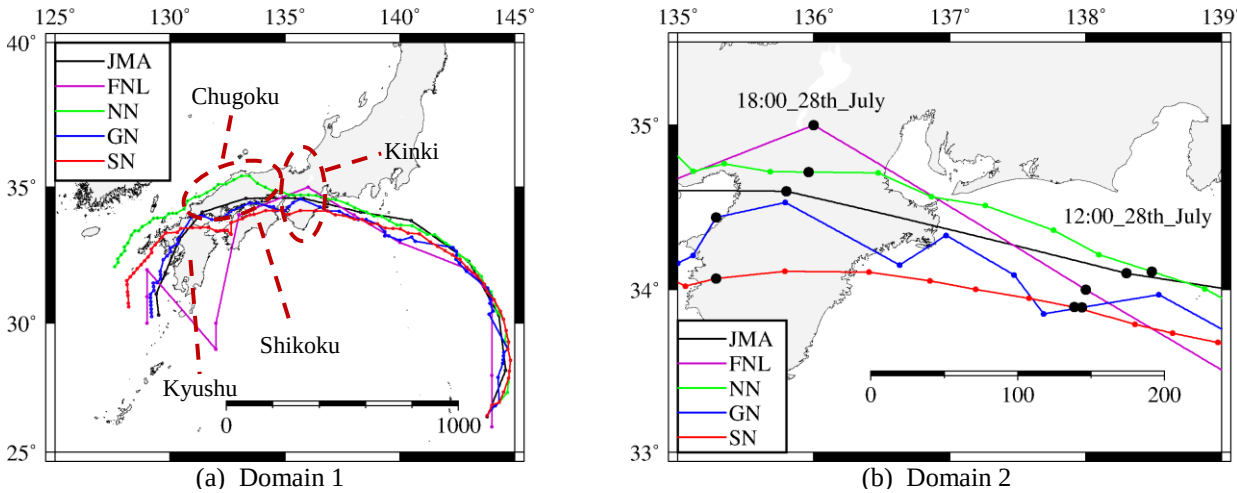

(a) Domain 1 (b) Domain 2

Figure 3. Typhoon tracks by observation and simulation

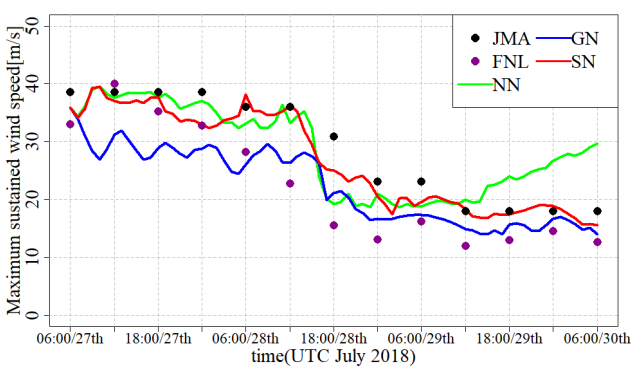

Figure 4. Maximum wind speed

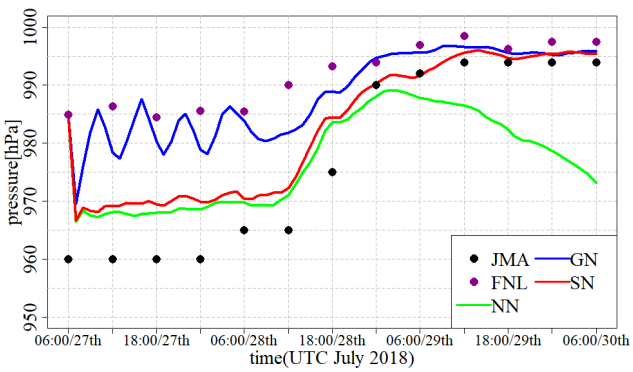

Figure 5. Lowest pressure

of maximum wind speed by GN was not enough. The wind speed by NN and SN at 12:00 28th July is similar to JMA. NN declines by about 13 m/s and SN declines by about 10 m/s between 12:00 and 18:00 on 28th July. The decrease in wind speed by SN is closer to JMA than other case. Therefore, the maximum wind speed of the typhoon by SN is closest to JMA.

The time history of typhoon's lowest pressure is shown in Figure 5. NN approaches JMA by 00:00 29th July, but after that time it is overestimated (lower) than JMA. It is considered that this overestimation was caused by the track of NN. The typhoon in NN arrived at the coast line of Chugoku district facing to the Japan Sea (Figure 3 (a)) and became stronger again due to the influence of sea area. The error of typhoon track caused the significantly different in maximum wind speed and lowest pressure from JMA results. SN is about 10 hPa higher than JMA until the storm surge would take the maximum around 18:00 28th July. This underestimation started from the beginning of the simulation and continued by 00:00 29th July as same as the result of NN. When the estimation of typhoon is focused, it is necessary that the pressure be improved. However, when focusing storm surges, it is within the allowable margin of error for the following reasons:

-Improvement in the estimation of typhoon lowest pressure is necessary for the research on typhoon characteristics. However, the main purpose of this research is reproduction of storm surge. And Theoretically, the 10 hPa decrease of pressure causes about 10 cm sea level rise. The deviation over one meter will be a serious storm surge disaster. Therefore, a difference of 10 cm in storm surge simulation would not be a significant error.

-In other researches on storm surge simulation using the meteorological model and storm surge model, the difference of 10 hPa or more between simulation result and observation are demonstrated even though a good agreement in storm surge simulation is indicated (e.g., Iwamoto et al., 2014; Mori et al., 2014; Nakamura et al., 2015). Therefore, the result by SN is practically sufficient.

Hence, the GN method can demonstrate the track closest to the JMA, but the reproducibility of the typhoon characteristics using SN method is better than the cases by GN and NN.

4.3 Sea Level Departure by Storm Surge

Figure 6 compares simulation and observation for tide level deviations, which is non-tidal sea level residuals, by storm surge. In NN, maximum departure is underestimated and its occurrence time delays at all stations. In the case of Morozaki, GN almost fits observation and SN overestimates. In other locations, SN almost fits observation and GN underestimate. Before the maximum departure at Mikawa, there are a large drop in the departure. Sufficient reproducibility of the large drop in NN and SN is demonstrated. Two apparent peaks of water surface rise were observed at Fukue around 15:00 and 18:00. SN shows the same tendency, but the calculated peak was milder and earlier than observed one. These two peaks are unique compared to other locations and are indicated at only Fukue. Figure 7 shows geographical features and FVCOM domain around Fukue. Fukue is a water area with a depth of less than 1 m and has a complicated topography. Moreover, the observation point is located inside the fishing port. Therefore, it is speculated that this topographic feature around Fukue observation point resulted in the less reproducibility of the first peak in simulations. Furthermore, it will be hard to improve the reproducibility of the first peak even if the topographic data is made with high resolution around Fukue observation point because topographic complexity and very shallow water depth condition will not be suitable for the simulation. From the viewpoint of estimation of highest and lowest departures, the result of non-tidal sea level fluctuation by SN is better than other cases.

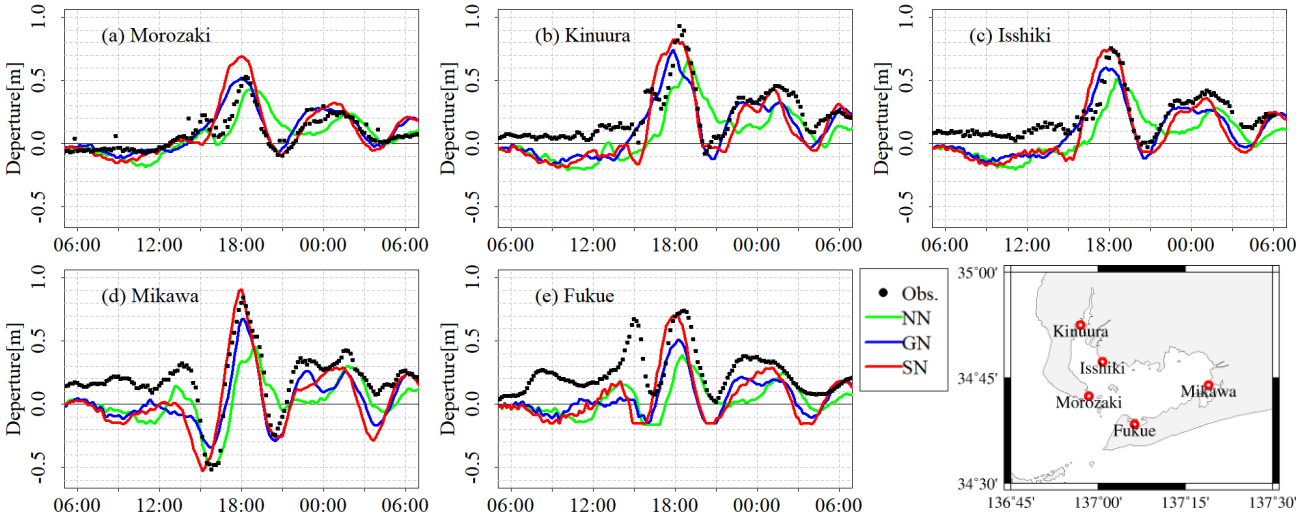

Figure 6. Sea level departure by storm surge without tide (Period is from 6:00 UTC 28th July 2018 to 6:00 UTC 29th July 2018)

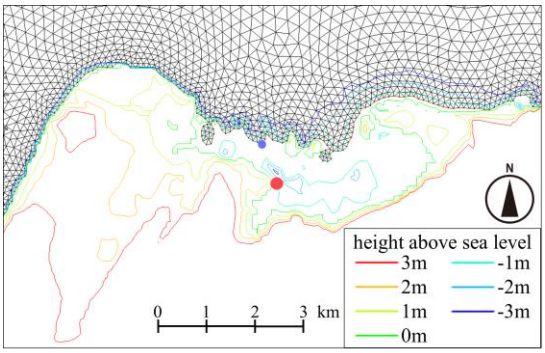

Figure 7. Geographical features (Central Disaster Management Council, 2016) and FVCOM domain around Fukue (● (red): location of tide station, ● (blue): FVCOM output)

The distribution of the current and the sea level departure by the typhoon of SN were analyzed. Figure 8 shows the distribution of the flow magnitude with the vector (left) and that of the sea level departure with the wind vector (right) during the typhoon passing. At 14:00, a wind from the north and the east caused flows from Mikawa Bay to Ise Bay, and from Ise Bay to ocean. Hence, the sea level departure of these bays decreased (change to cold colors) between 14:00 and 15:00. It caused a large decrease in the departure before the maximum departure at Mikawa (Figure 8(b)). However, at 15:00, the typhoon in south of the bays inlet (Figure 3(b)) generated an east wind on the bays. By the north wind weakening, water pushed out of the bays by the north wind during typhoon approaching would flow back into Ise Bay in Figure 8(c). From 17:00 to 17:30 (Figure 8 (d) and (e)), the sea level departure reached the peak at Ise Bay and a flow from ocean to Mikawa Bay through Ise Bay was generated. First, water from ocean flows into Ise Bay. And when enough water accumulated in Ise Bay, water from ocean then flows into Mikawa Bay. The difference of occurrence time of maximum water level between Ise Bay and Mikawa Bay will be considered to be a characteristic phenomenon that occurs in two connected bays. After that, at 18:00, a sea level departure peaked at Mikawa Bay.

When the typhoon with reverse track, as Jongdari, approaches or passes, it is speculated that sea level decrease at Ise Bay and Mikawa Bay. However, after the typhoon passed by their bays, there is the rapidly increase in the sea level departure. Thus, not only when the typhoon approaches or passes, it requires watching for storm surge after the typhoon passed.

5. SUMMARY

Typhoon Jongdari is the first record of the reverse track around Japan. This track has not

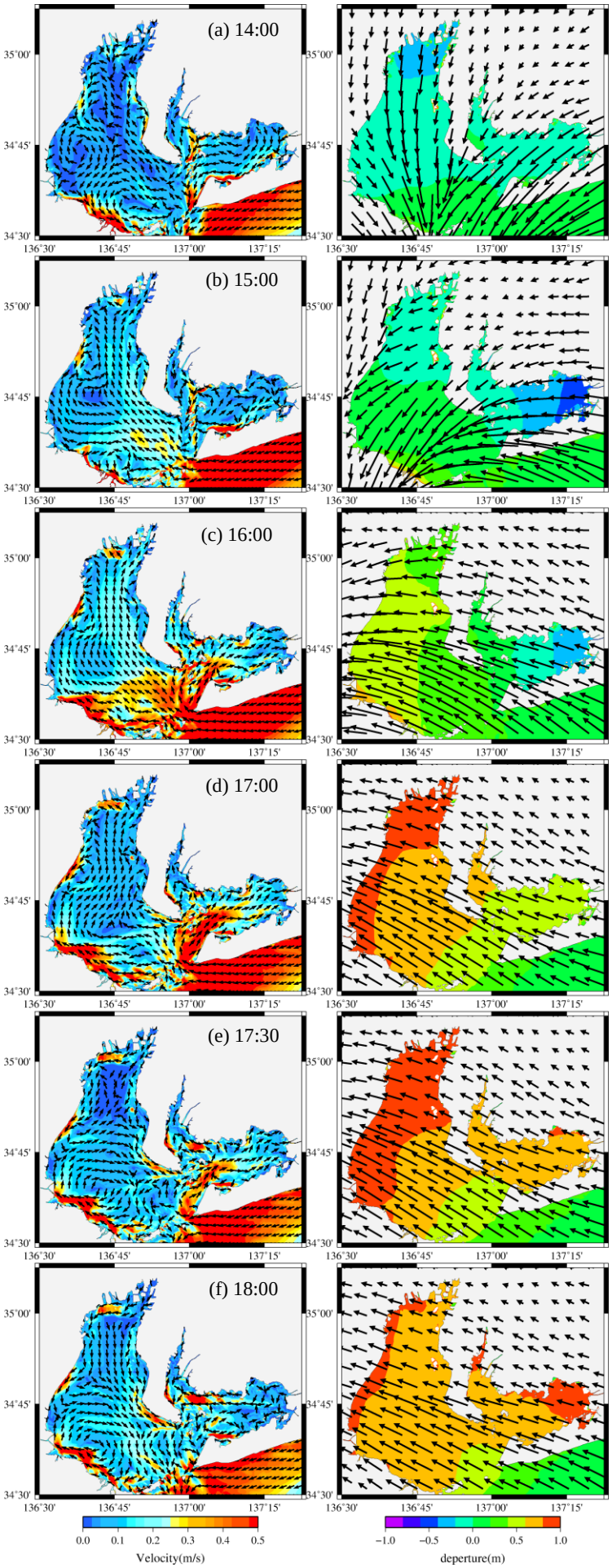

Figure 8. Spatial distribution changes of flow vector and magnitude, and water level departure in Ise Bay and Mikawa Bay in SN

been assumed for storm surge disaster prevention at present. The improvement of reproducibility of storm surge numerical calculations for this typhoon and elucidation of storm surge generation mechanism are necessary for strengthening measures against coastal disaster in the future. In this study, we examined the effectiveness of four-dimensional data assimilation on the reproduction of Typhoon Jongdari and its storm surge deviation using atmospheric model (WRF) and ocean flow model (FVCOM). In addition, we examined the generation mechanism of storm surge deviation. From the results and observations obtained, the following conclusions were drawn:

1. The typhoons by GN are closer to JMA (Best Track) than NN and SN. However, its strength is weaker than other case typhoon. Therefore, it is assumed that the reproducibility of typhoon and storm surge be not sufficient. On the other hands, SN demonstrates the typhoon strength and storm surge departure by observation appropriately. Therefore, it appears that the grid nudging method can reproduce the typhoon track adequately than the spectral nudging and the method using spectral nudging is a suitable method to demonstrate high reproducibility of storm surge departure.
2. When the typhoon with reverse track, as Jongdari, approaches to Ise Bay and Mikawa Bay or passes through these bays, a northeast wind causes the flows from Mikawa Bay to Ise Bay, and from Ise Bay to ocean. As a result, it is speculated that sea level decrease at their bays. However, after the typhoon passed by their bays, the southeast wind causes the flows from ocean to Ise Bay. Further, seawater accumulated in Ise Bay flows into Mikawa Bay. As a result, there is the rapidly increase in the sea level departure by storm surge.

ACKNOWLEDGMENTS

This research was parts of the project for study on air-sea interaction and process of RI typhoon (MOF).

REFERENCES

Central Disaster Management Council. (2016). Tsunami Fault Model (5) Topographic data. [https://www.geospatial.jp/ckan/dataset/1205]. accessed May 2018.

Chen, C., Liu, H. and Beardsley, R. C. (2003). An Unstructured Grid, Finite-Volume, Three-Dimensional, Primitive Equations Ocean Model: Application to Coastal Ocean and Estuaries, *Journal of Atmospheric and Oceanic Technology*. vol. 20(1). pp. 159-186.

Guiney, L., J. (1999), Preliminary Report Hurricane Lenny 13 - 23 November 1999. *National Hurricane Center*, [https://www.nhc.noaa.gov/data/tcr/AL161999_Lenny.pdf] accessed 31 January 2020.

Iwamoto, T., Nakamura, R., Oyama, T., Mizukami, R and Shibayama, T. (2014), Prediction of Storm Surge at Tokyo Bay under RCP 8.5 Scenario by Using Meteorological-Surge-Tide Coupled Model. *Proceedings of Coastal Engineering*. Japan Society of Civil Engineers, vol. B2-70. pp. 1261-1265.

Janjic, Z. I. (2003). A nonhydrostatic model based on a new approach. Meteorol. Atoms. Phys. 82, pp. 271-285.

Kato, S., Dinh, V. V., LE, D. Q. and Okabe, T. (2014), Formative Mechanism of High Water Level Region in Chita Bay due to Storm Surge in Mikawa Bay. *Proceedings of Coastal Engineering*. Japan Society of Civil Engineers, vol. B2-70. pp. 251-256.

Myers, V. A., and Malkin, W. (1961), Some properties of hurricane wind fields as deduced from trajectories. Natinal Hurricane Research Project, U.S. Department of Commerce, Weather Bureau, Report 49.

Mori, N., Shibutani, Y., Takemi, T., Kim, S., Yasuda, T., Niwa, T., Tsujio, D. and Mase, H. (2014), Forecast and Hindcast of Storm Surge Modeling by Typhoon Haiyan in 2013. *Proceedings of Coastal Engineering*. Japan Society of Civil Engineers, vol. B2-70. pp. 246-250.

Murakami, T., Yoshino, J., Fukao, H. and Yasuda, T. (2013), Unexpected Storm Surge Caused in Mikawa Bay and Its Generation Mechanism. *Proceedings of Coastal Engineering*. Japan Society of Civil Engineers, vol. B2-69. pp. 221-225.

Nakamura, R., Oyama, T., Shibuyama, T., Miguel, E. and Takagi, H. (2015). Evaluation of Storm Surge Caused by Typhoon Yolanda (2013) and Using Weather – Storm Surge – Wave – Tide Model. *Procedia Engineering*, 116. pp.373-380.

NCAR. (1999), NCEP FNL Operational Model Global Tropospheric Analyses. continuing from July 1999. [https://rda.ucar.edu/datasets/ds083.2/] accessed 31 January 2019.

Powell, M. D., Vickery, P. J. and Reinhold, T. A. (2003). Reduced drag coefficient for high wind speeds in tropical cyclones. *Nature*. 422. pp. 279-283.

Skamarock, W. C., Klemp, J. B., Duddhia, J, Gill, D. O., Barker, D. M., Duda, M. G., Huang, X. Y., Wang, W. and Ouwers, J. G. (2008). A Description of the Advanced Research WRF Version 3. NCAR TECHNICAL NOTE.

Yasuda, T., Yamaguchi, T., Kim, S. Y., Shimada, H., Ishigaki, T. and Mase, H. (2008). Numerical Study of Storm Surge Hindcast Simulations in the Seto Inland Sea by Surge-Wave-Tide Coupled Model and Mesoscale Atmospheric Model WRF. *Proceedings of Coastal Engineering*. Japan Society of Civil Engineers, vol. 55. pp. 331-335.

Yasuda, T., Yamaguchi, T., Kim, S. Y., Mori, N. and Mase, H. (2009). Effectiveness of 4-Dimensional Data Assimilation and Nesting in an Atmospheric Model on Accuracy of Storm Surge Predictions. *Proceedings of Coastal Engineering*. Japan Society of Civil Engineers, vol. B2-65. pp. 381-385.

Yuu, H., Ohsawa, T., Kozai, K., Yamaguchi, A., Ishihara, T. and Nakano, T. (2012). A study on calculation method in typhoon wind simulation with WRF. *Proceedings of National Symposium on Wind Engineering*. Japan Association for Wind Engineering. No. 22. pp. 383-388

Wu, J. (1980). Wind-Stress coefficients over Sea surface near Neutral Conditions—A Revisit. *American Meteorological Society*. pp. 727-740.